

# THz Higher-Order Topological Photonics in Ge-on-Si Heterostructures

Ian Colombo<sup>1</sup>, Pietro Minazzi<sup>1</sup>, Emiliano Bonera<sup>1</sup>, Fabio Pezzoli<sup>1\*</sup> and Jacopo Pedrini<sup>1</sup>

<sup>1</sup> Dipartimento di Scienza dei Materiali, Università degli Studi di Milano-Bicocca and BiQuTe, via R. Cozzi 55, 20125 Milan (Italy)

\* [fabio.pezzoli@unimib.it](mailto:fabio.pezzoli@unimib.it)

## Abstract

We design germanium-based higher-order topological cavities for terahertz applications by breaking the symmetry of a two-dimensional photonic crystal following the Su-Schrieffer-Heeger model. Calculations demonstrate the parity inversion of the electric field in differently deformed unit cells. The interface between domains of opposite topology presents edge and corner modes. The former are chiral, locking light propagation to its helicity. The latter prove that Ge-based structures can be used as high-order topological photonic crystals. These findings can accelerate the development of Si-photonics components working in a spectral range of high technological interest.

Copyright attribution to authors.

This work is a submission to SciPost Physics.

License information to appear upon publication.

Publication information to appear upon publication.

Received Date

Accepted Date

Published Date

1

## 2 Contents

3	<b>1 Introduction</b>	<b>1</b>
4	<b>2 Results and discussion</b>	<b>2</b>
5	<b>3 Conclusions</b>	<b>6</b>
6	<b>References</b>	<b>8</b>

7

8

## 9 1 Introduction

10 The comprehension and exploitation of the topological properties of matter led to the emer-  
 11 gence of research on topological insulators [1] and their photonic analogs, known as topo-  
 12 logical photonic crystals (TPC). [2, 3] TPCs have been shown to be promising for the fabrica-  
 13 tion of photonic integrated circuits thanks to exceptional features, e.g., directional and chiral  
 14 light propagation, [4–6] strong resistance to sharp bends, [7] and mathematical protection

15 from defect-induced scattering. [8] These properties are indeed expected to facilitate the im-  
16 plementation of advanced photonic components such as directional, polarization-dependent  
17 waveguides, [9–11] resonators, [12] drop-filters [13] and topological lasers. [7, 14, 15]

18 Lately, higher-order topology has been gaining attention in photonics research. In con-  
19 trast to conventional topological insulators, higher-order topological insulators (HOTI) present  
20 conductive states that are more than one dimension lower than the insulating state. [16, 17]  
21 This has led to the concept of special two-dimensional (2D) TPCs, which can feature unusual  
22 zero-dimensional (0D) corner states in addition to the conductive one-dimensional (1D) hinge  
23 modes. The potential to exploit HOTIs to fully confine the electromagnetic field at a 0D cor-  
24 ner and topologically protect it from undesired losses is fundamentally intriguing and strongly  
25 appealing for applications, particularly because it might drastically boost lasing emission and  
26 improve spectral purity. [14]

27 Although crystals with a trivial photonic band structure have already found applications in  
28 the terahertz (THz), [18, 19] the extension of HOTIs into such frequency range has been very  
29 limited thus far. The interest in this spectral regime comes from the inherent capacity to stream  
30 high-frequency wide-bandwidth data; [20] a characteristic that offers significant prospects for  
31 the advancement of wireless communication networks beyond existing 5G standards. [21, 22]  
32 In addition to telecommunications, THz waves can have far-reaching consequences in various  
33 fields, including quantum information, [21–23] non-destructive imaging, [24, 25] biological  
34 sensing and diagnostics, [26, 27] security and defense. [28, 29] The development of efficient  
35 THz photonic components and devices is thus a compelling task where TPC and HOTIs can  
36 provide a leap forward with novel and yet untapped capabilities.

37 Another crucial factor in achieving this ambitious goal is the choice of materials platform  
38 that can favor an industrial takeover while being, at the same time, suitable for the THz regime.  
39 Germanium stands out as a solution to these two problems since it offers a transparency win-  
40 dow that is spectrally broad, [30, 31] while being already present in microelectronic and pho-  
41 tonic foundries. Ge-based high-quality photonic crystals (PC) can be indeed created using  
42 conventional lithography and vertical etching of thin Ge-on-Si films [32–34] or by exploiting  
43 self-assembly of Ge crystals directly on top of patterned Si substrates. [35] This can result in  
44 high-volume production and opens the route toward monolithic integration of THz photonic  
45 components into Si chips.

46 So far, literature reports have shown that Ge-on-Si heterostructures host promising, albeit  
47 non-topological, photonic properties in the near-infrared region of the electromagnetic spec-  
48 trum. [36–38] To unfold the Ge potential in exhibiting HOTI states in the THz regime, we  
49 employ the finite elements method (FEM) to investigate photonic and topological properties  
50 including the emerge of a photonic band gap (PBG) and the topology-induced spatial confine-  
51 ment and directional propagation of light. In this work, we will concentrate on the model  
52 system offered by the self-assembly of micron-sized Ge-on-Si rods. Their typical in-plane ar-  
53 rangement can seemingly mimic 2D TPCs with a square geometry [14, 39–43] and their distinct  
54 optical properties [44–48] can possibly expedite the practical realization of future, integrated  
55 HOTI devices.

## 56 2 Results and discussion

57 Figure 1a shows the layout of a typical microstructure consisting of Ge-on-Si microcrystals. To  
58 determine the photonic bandstructure of the 2D lattice as close as possible to the experimental  
59 ones, [37] we simulated a unit cell composed of a pseudo-octagonal Ge microcrystal, featuring  
60 both {100} and {111} facets surrounded by vacuum. The lattice parameter is  $a = 2 \mu\text{m}$  to  
61 ensure experimental feasibility with conventional fabrication processes. [37] The size  $d$  of the

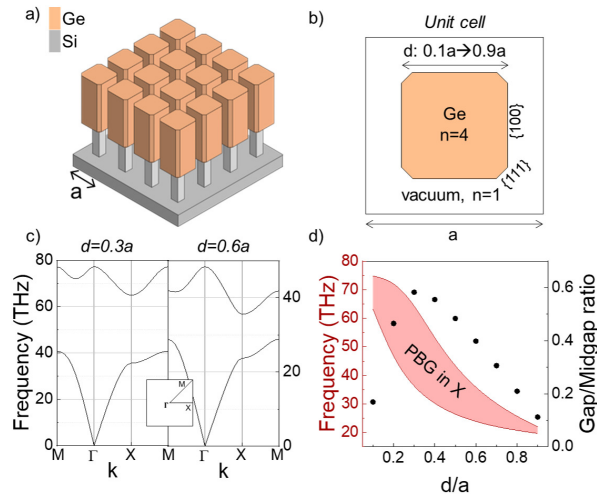


Figure 1: a) Sketch of the model photonic crystal (PC) based on a Ge (orange) on Si (grey) heterostructure (not to scale). [37] The lattice parameter is  $a$ . b) Scheme of the simulated unit cell of the PC. c) Simulated bandstructure of the PC calculated using finite element method for a Ge crystal size  $d = 0.3a$  (left) and  $d = 0.6a$  (right). Inset: Irreducible Brillouin Zone of the square lattice with high symmetry points indicated. d) Size of the photonic bandgap (PBG) calculated in the  $X$  point of the bandstructure (red shaded area) and gap/midgap ratio (black dots) as a function of  $d$ .

62 Ge microcrystal was varied in the FEM calculations between  $0.1a$  and  $0.9a$ . The refractive  
 63 index of Ge has been extracted from the literature [49] and is  $n \sim 4$ , corresponding to the  
 64 value measured in the THz region of the electromagnetic spectrum, where the extinction coef-  
 65 ficient is zero and  $n$  itself can be considered constant for the purposes of the calculations. The  
 66 geometry of the unit cell, together with the structure parameters, is reported in Figure 1b.

67 We performed a FEM simulation of the system eigenfrequencies with Comsol Multiphysics  
 68 [50], using Floquet periodicity and varying the size  $d$  of the microcrystal to gather information  
 69 on the optimal geometric parameters of the PC. The simulation was performed for the out-  
 70 of-plane electric field configuration, also known as transverse magnetic (TM) modes. The  
 71 simulation sweeps the wavevector  $k$  along high symmetry directions in the irreducible Brillouin  
 72 Zone (IBZ), yielding the photonic bandstructure that is reported in Figure 1c for two values  
 73 of  $d$ , namely  $d = 0.3a$  and  $d = 0.6a$ , corresponding to a microcrystal lateral size of 600 nm  
 74 and 1200 nm, respectively. The calculated bandstructures for every value of  $d$  are reported in  
 75 the Supplementary Material. The bandstructures present a large PBG in the THz region of the  
 76 electromagnetic spectrum.

77 The bandstructures have similar shapes for different values of  $d$ , but its increase shifts the  
 78 energy bands toward lower frequencies and apparently shrinks the amplitude of the PBG as  
 79 shown in Figure 1d, which reports the size of the PBG at the  $X$  high-symmetry point of the  
 80 IBZ as a function of  $d$ . The size of the gap increases with  $d$  and then decreases until it is  
 81 almost negligible. This behavior is expected in 2D PCs dominated by a high refractive index  
 82 material. [51] To compare the size of the PBG between the different structures, we normalized  
 83 the bandgap to the midgap frequency. This renormalization method allows us to compare the  
 84 relative amplitude of the PBG in structures with different geometries. [51] The calculation of  
 85 the gap/midgap ratio in our case yields that the structure with the largest bandgap is that  
 86 with  $d = 0.3a$ . Unless otherwise noted, hereafter we refer to this specific value of  $d$  (results  
 87 obtained for  $d = 0.6a$  are nonetheless reported in the Supplementary Material).

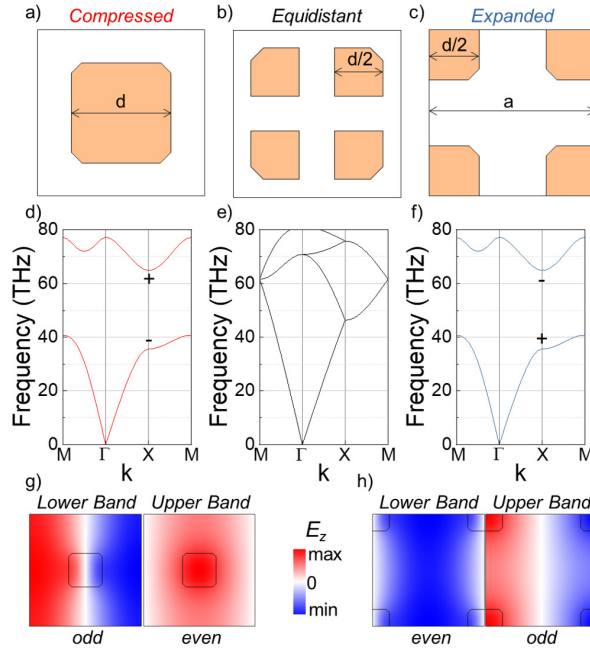


Figure 2: Scheme of the unit cell, simulated photonic bandstructure, and electromagnetic field distribution for the compressed (a,d,g), equidistant (b,e) and expanded (c,f,h) PCs when the lateral size of the Ge crystal  $d$  equals 0.3 times the lattice parameter  $a$ . The out-of-plane component of the electromagnetic field (TM mode) is computed at the  $X$  point of the IBZ. The parity of the wavefunction acts as a pseudospin, and the symmetry inversion (indicated by the + and -) between the compressed and the expanded crystals is the fingerprint of a topological phase transition.

88 It should be noted that the photonic properties of the simulated system depend on the spe-  
 89 cific value of the lattice parameter  $a$ . However, the scaling invariance allows one to rigidly shift  
 90 the energy of the PBG towards lower (higher) frequencies just by fabricating larger (smaller)  
 91 unit cells. This powerful property provides great flexibility because it allows structures with a  
 92 PBG in resonance with a desired frequency, e.g., the emission frequency of a quantum cascade  
 93 structure. There are reports in the literature [52, 53] showing Ge/SiGe MQWs with interband  
 94 emission at  $\sim 30$  THz, a value that can already be reached with the PC described in Figure 1,  
 95 e.g. for  $d = 0.8a$ . The structure can be further optimized by setting  $d = 0.3a$ , where the PBG  
 96 is the largest, and increasing the lattice parameter  $a$  by a factor  $\sim 2$ .

97 The 2D lattice composed of the semiconductor microcrystals can be seen as the periodic  
 98 repetition of two different unit cells. The two structures can be considered the extreme case  
 99 of a photonic extension of a 2D Su-Schrieffer-Heeger (SSH) lattice, [40, 54, 55] where a unit  
 100 cell composed of four elements equidistant from both the center and the vertex of the cell is  
 101 distorted, as shown in Figure 2. The first unit cell has a microcrystal with lateral size  $d$  at  
 102 the center of the cell, as shown in Figure 1b or Figure 2a, and will from now on be referred  
 103 to as *compressed*. The other structure consists of four quarters of a microcrystal with a width  
 104  $\frac{d}{2}$  placed at the corners of the cell, as shown in Figure 2c. We will refer to this structure as  
 105 *expanded*. The *equidistant* unit cell structure is reported in Figure 2b.

106 The bandstructures of the described lattices are reported in Figure 2d-f. The one of the *equidis-*  
 107 *tant* PC (reported in Figure 2e) is gapless and shows a pseudo-Dirac point at the  $M$  and  $X$   
 108 high-symmetry points. The deformation of the unit cell opens a gap, as expected in the SSH  
 109 model, and yields two identical photonic bandstructures for the *compressed* and *expanded* PCs.

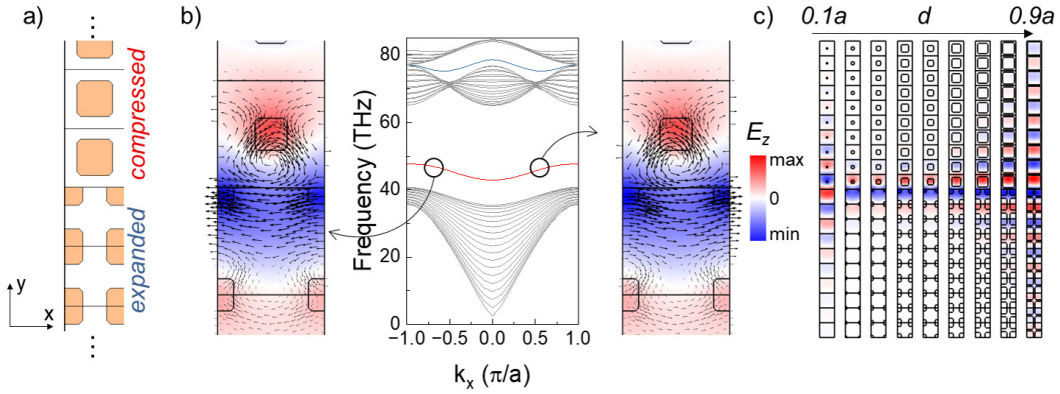


Figure 3: a) Schematics of a supercell consisting of a line interface between a compressed and expanded PCs. b) Calculated bandstructure of the supercell along the  $x$  direction. The bandstructure presents bulk bands (grey) with two sizeable gaps in which localized modes are present (red and blue curves). The modes are confined at the interface of the two regions of the PCs. The arrows overlaid on the electromagnetic field distribution underline the directionality of the propagation. c) Spatial distribution of the out-of-plane component of the electromagnetic field ( $E_z$ ) in the supercell as a function of the lateral size of Ge  $d$ . The supercells are stacked horizontally as  $d$  increases from  $0.1a$  to  $0.9a$ , where  $a$  is the lattice parameter.

110 It is important to highlight that in a SSH model the band dispersion does not change with  
 111 the inversion of the intra- and inter-cellular distances between the elements composing the  
 112 unit cell, but the symmetry of the eigenfunctions is different, as they possess opposite parity.  
 113 [40, 55] To gather further insights on the bandstructure of the *expanded* and *compressed*  
 114 PCs, we calculated the out-of-plane electric field distribution  $E_z$  (TM mode) for such unit cells.  
 115 Particularly, we investigate the  $E_z$  distribution at the X point of the bandstructure, where the  
 116 PBG opens up. The  $E_z$  distribution maps are reported in Figure 2g,i. Here, the *compressed* PC  
 117 presents an even  $E_z$  distribution in the lower band and an odd distribution in the high-energy  
 118 band. The opposite occurs in the *expanded* structure. This parity inversion confirms the equiv-  
 119 alence of the two PC structures to a 2D SSH model. Therefore, the *compressed* and *expanded*  
 120 PC belongs to distinct topological phases, where the parity of the bands can be considered as  
 121 the topological invariant. In particular, the *compressed* structure is an ordinary insulator, while  
 122 the *expanded* is topologically nontrivial.

123 The clearest evidence of the presence of a topological transition is the emergence of spa-  
 124 tially confined guided modes at the boundary between two domains with different band topol-  
 125 ogy. [5, 7, 56–58] Figure 3a reports the schematic of an interface between the two PCs char-  
 126 acterized by distinct topological invariants. For its characterization we designed a so-called  
 127 *supercell* composed of a ribbon of 20 unit cells where the top (bottom) 10 unit cells are *com-*  
 128 *pressed* (*expanded*). In other words, the top half of the supercell is an ordinary insulator, while  
 129 the bottom half is topologically nontrivial. The FEM simulation of this structure is performed  
 130 with periodic conditions along the  $x$  direction, and the eigenfrequencies are calculated as a  
 131 function of  $k_x$ , from  $-\frac{\pi}{a}$  to  $\frac{\pi}{a}$ . A perfectly matched layer is used as the boundary condition  
 132 for the top and bottom of the ribbon to simulate an infinite PC. The resulting bandstructure is  
 133 shown in Figure 3b. It presents a large number of bulk modes and two energy gaps, the larger  
 134 of which covers the interval between 41 and 65 THz, while a second, non complete one is at  
 135 around 75 THz. For the scope of this work, we focus on the full PBG at lower energy. The  
 136 bandgap frequencies are the same as those calculated for the bulk unit cells along the  $\Gamma - X$   
 137 direction (see Figure 2). The presence of a single mode in the PBG, located at  $\sim 45$  THz, is a

138 fingerprint of the interface of two phases with a different topological invariant. Such a mode is  
139 spatially localized at the interface of the two domains, as is shown by the plot of  $E_z$  (see Figure  
140 3b), with the electric field mostly penetrating the high-index structure. The arrows overlaid  
141 on the  $E_z$  map are the local Poynting vectors that represents the direction of propagation of the  
142 electromagnetic wave. The representation of the Poynting vector allows us to underline the  
143 presence of unidirectional propagating modes, that can be selectively coupled through helical  
144 excitation. [3, 5, 56] Figure 3c shows that when  $d$  is varied the imbalance between the air and  
145 Ge fractions affects the confinement of the edge mode, so that the field is almost perfectly  
146 localized within the two interfacial unit cells only for  $d$  ranging from  $0.2a$  to  $0.5a$ .

147 The demonstration of the presence of optical modes at the interface between domains  
148 suggests a possible application of Ge-on-Si photonic architectures as on-chip THz waveguides  
149 in topological circuits. We can further extend our results by designing a 2D device that could  
150 also exploit the generation of higher-order topological modes at the intersection between such  
151 hinge modes. Figure 4a introduces a resonator composed of a square of the *expanded* PC having  
152 a side of 9-unit cells, surrounded by a cladding frame consisting of 4-unit cells of the *compressed*  
153 PC defining an interface that supports the mode described in Figure 3. The solutions of the  
154 eigenvalue analysis for the resonator are separated in four well-defined frequency regions, as  
155 shown in Figure 4b,c. The nature of these modes can be determined by analyzing the electric  
156 field distribution, as shown in Figure 4d-g. The electromagnetic field maps for solutions for  
157 frequencies  $< 41$  THz (see Figure 4d) and  $> 65$  THz (see Figure 4g) clearly demonstrate  
158 the bulk nature of the modes, that permeate vast regions of the PC. In the frequency range  
159 pertaining to the PBG two well separated sets of solutions are present at  $\sim 47$  THz and at  $55$   
160 THz. First, we focus on the four degenerate modes at  $55$  THz that dominate the energy density  
161 spectrum reported in Figure 4c. The map of the electric field distribution, reported in Figure  
162 4f, shows that these are extremely localized OD corner modes. Their existence demonstrates  
163 that the structure described in this work is a higher-order TPC characterized by a bulk-edge-  
164 corner correspondence. [59] Moreover, localized corner modes are extremely interesting for  
165 their strong confinement properties and can be exploited for their possible applications to  
166 devices that need high-quality factor resonators such as light emitters, sensors, and non-linear  
167 systems. [40, 41, 60, 61]

168 We now focus on the lower energy modes, found at frequency around  $47$  THz. The electro-  
169 magnetic field distribution shows that these are edge modes confined at the interface between  
170 the trivial and topological PC structures. Their study can give further insight on the topological  
171 properties of the PC and how they influence the propagation of light at the interface between  
172 the two topologically-distinct domains. As described above, a characteristic property of TPCs  
173 is the directional propagation of light, which is related to its degree of circular polarization. To  
174 demonstrate this feature, we simulated the propagation of circularly polarized light by using  
175 an array of opportunely spaced phased dipoles localized at the interface between the topologi-  
176 cally distinct regions. [62] The overlay of the Poynting vector on the electromagnetic field map,  
177 shown in Figure 4h-i, demonstrates how the propagation is strongly directional and locked to  
178 the degree of circular polarization, allowing chiral propagation at the interface of the PCs in  
179 the THz range.

### 180 3 Conclusions

181 We demonstrated the possibility of achieving higher-order topological effects in the THz regime  
182 in a PC composed of group IV heteroepitaxial microstructures. Such a HOTIs can be utilized  
183 for the development of elemental components of photonic circuitries such as resonators and  
184 waveguides. By combining Ge-based heterostructures with the intrinsic scalability of PCs one

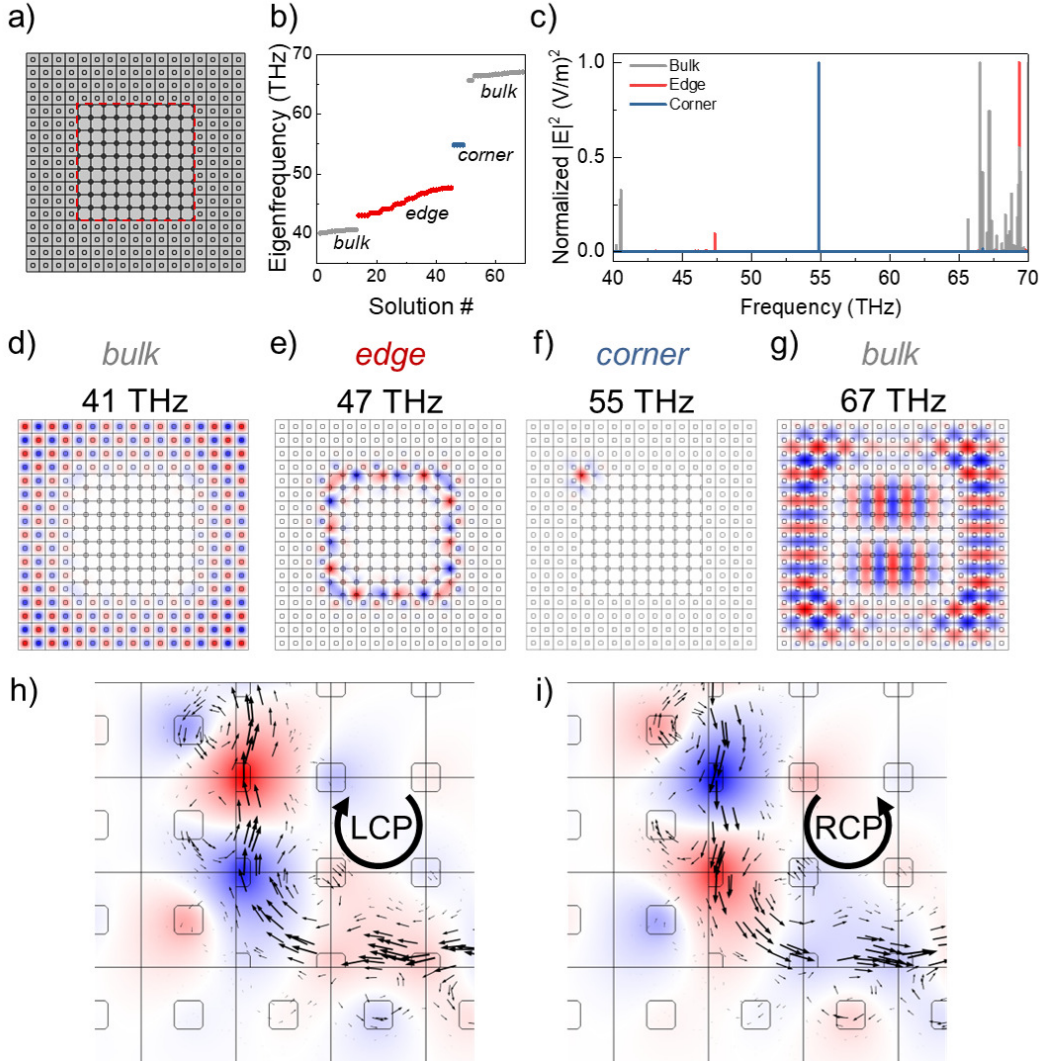


Figure 4: a) Schematics of a resonator composed of a square interface between an expanded PC surrounded by a compressed PC ( $d = 0.3a$ ). The interface is marked with a red dashed line. b) Eigenfrequency values of the resonator as a function of the solution number. Four groups can be identified that correspond to bulk modes (low- and high-energy, grey), edge (red), and corner (blue) modes. c) Normalized field intensity as a function of the frequency, highlighting the bulk, edge and corner modes. d-g) Distribution of the out-of-plane component of the electric field at four significant frequencies corresponding to a low-energy bulk mode (d), edge mode (e), corner mode (f), and a high-energy bulk mode (g). h,i) Electromagnetic field  $E_z$  distribution at the bottom left corner of the resonator, when the resonator is excited with left (h) and right (i) circularly polarized light. The arrows at the interface between the topologically distinct regions are the Poynting vectors, highlighting a direct correspondence between light polarization and the direction of propagation.

185 can obtain devices working in a wide range of frequencies, possibly from mid-infrared to the  
186 THz. Furthermore, the capacity to embed THz emitters in the microstructures in the form of  
187 Ge/SiGe quantum wells might open a pathway to realize integrated, topological lasers with  
188 a small footprint and high throughput that operate within technologically relevant spectral  
189 regions.

## 190 Acknowledgements

191 The authors thank A. Marzegalli for technical assistance and L. Miglio for fruitful discussions.

192 **Funding information** This work has been funded by the European Union's Horizon Europe  
193 Research and Innovation Programme under agreement 101070700. Support from PNRR MUR  
194 project PE0000023-NQSTI is also acknowledged. J.P. acknowledges financial support from  
195 FSE REACT-EU (grant 2021-RTDAPON-144).

## 196 References

- 197 [1] M. Z. Hasan and C. L. Kane, *Colloquium: Topological insulators*, *Reviews of Modern*  
198 *Physics* **82**(4), 3045 (2010), doi:[10.1103/RevModPhys.82.3045](https://doi.org/10.1103/RevModPhys.82.3045).
- 199 [2] L. Lu, J. D. Joannopoulos and M. Soljačić, *Topological photonics*, *Nature Photonics* **8**(11),  
200 821 (2014), doi:[10.1038/nphoton.2014.248](https://doi.org/10.1038/nphoton.2014.248), [1408.6730](https://doi.org/10.1038/1408.6730).
- 201 [3] T. Ozawa, H. M. Price, A. Amo, N. Goldman, M. Hafezi, L. Lu, M. C. Rechtsman, D. Schus-  
202 ter, J. Simon, O. Zilberberg and I. Carusotto, *Topological photonics*, *Reviews of Modern*  
203 *Physics* **91**, 015006 (2019), doi:[10.1103/RevModPhys.91.015006](https://doi.org/10.1103/RevModPhys.91.015006).
- 204 [4] P. Lodahl, S. Mahmoodian, S. Stobbe, A. Rauschenbeutel, P. Schneeweiss, J. Volz,  
205 H. Pichler and P. Zoller, *Chiral quantum optics*, *Nature* **541**(7638), 473 (2017),  
206 doi:[10.1038/nature21037](https://doi.org/10.1038/nature21037), [1608.00446](https://doi.org/10.1038/1608.00446).
- 207 [5] L. H. Wu and X. Hu, *Scheme for achieving a topological photonic crys-*  
208 *tal by using dielectric material*, *Physical Review Letters* **114**(22), 1 (2015),  
209 doi:[10.1103/PhysRevLett.114.223901](https://doi.org/10.1103/PhysRevLett.114.223901).
- 210 [6] J. W. Dong, X. D. Chen, H. Zhu, Y. Wang and X. Zhang, *Valley photonic crystals for control*  
211 *of spin and topology*, *Nature Materials* **16**(3), 298 (2017), doi:[10.1038/nmat4807](https://doi.org/10.1038/nmat4807).
- 212 [7] Y. Zeng, U. Chattopadhyay, B. Zhu, B. Qiang, J. Li, Y. Jin, L. Li, A. G. Davies, E. H. Linfield,  
213 B. Zhang, Y. Chong and Q. J. Wang, *Electrically pumped topological laser with valley edge*  
214 *modes*, *Nature* **578**(7794), 246 (2020), doi:[10.1038/s41586-020-1981-x](https://doi.org/10.1038/s41586-020-1981-x).
- 215 [8] Z. Wang, Y. Chong, J. D. Joannopoulos and M. Soljačić, *Observation of unidirectional*  
216 *backscattering-immune topological electromagnetic states*, *Nature* **461**(7265), 772 (2009),  
217 doi:[10.1038/nature08293](https://doi.org/10.1038/nature08293).
- 218 [9] M. Jalali Mehrabad, A. P. Foster, R. Dost, E. Clarke, P. K. Patil, A. M. Fox, M. S. Skolnick  
219 and L. R. Wilson, *Chiral topological photonics with an embedded quantum emitter*, *Optica*  
220 **7**(12), 1690 (2020), doi:[10.1364/OPTICA.393035](https://doi.org/10.1364/OPTICA.393035).



- 221 [10] Y. Yang, Y. F. Xu, T. Xu, H.-X. Wang, J.-H. Jiang, X. Hu and Z. Hang, *Visual-*  
222 *ization of a unidirectional electromagnetic waveguide using topological photonic crys-*  
223 *tals made of dielectric materials*, Physical Review Letters **120**(21), 217401 (2018),  
224 doi:[10.1103/PhysRevLett.120.217401](https://doi.org/10.1103/PhysRevLett.120.217401).
- 225 [11] N. Parappurath, F. Alpeggiani, L. Kuipers and E. Verhagen, *Direct observation of topolog-*  
226 *ical edge states in silicon photonic crystals: Spin, dispersion, and chiral routing*, Science  
227 Advances **6**(10), eaaw4137 (2020), doi:[10.1126/sciadv.aaw4137](https://doi.org/10.1126/sciadv.aaw4137).
- 228 [12] M. Jalali Mehrabad, A. P. Foster, R. Dost, E. Clarke, P. K. Patil, I. Farrer, J. Heffernan, M. S.  
229 Skolnick and L. R. Wilson, *A semiconductor topological photonic ring resonator*, Applied  
230 Physics Letters **116**(6), 061102 (2020), doi:[10.1063/1.5131846](https://doi.org/10.1063/1.5131846).
- 231 [13] M. J. Mehrabad, A. P. Foster, N. J. Martin, R. Dost, E. Clarke, P. K. Patil, M. S. Skolnick and  
232 L. R. Wilson, *Chiral topological add-drop filter for integrated quantum photonic circuits*,  
233 Optica **10**(3), 415 (2023), doi:[10.1364/OPTICA.481684](https://doi.org/10.1364/OPTICA.481684).
- 234 [14] C. Han, M. Kang and H. Jeon, *Lasing at Multidimensional Topological States in*  
235 *a Two-Dimensional Photonic Crystal Structure*, ACS Photonics **7**(8), 2027 (2020),  
236 doi:[10.1021/acsp Photonics.0c00357](https://doi.org/10.1021/acsp Photonics.0c00357).
- 237 [15] Y. Ota, R. Katsumi, K. Watanabe, S. Iwamoto and Y. Arakawa, *Topological photonic crystal*  
238 *nanocavity laser*, Communications Physics **1**(1), 4 (2018), doi:[10.1038/s42005-018-](https://doi.org/10.1038/s42005-018-0083-7)  
239 [0083-7](https://doi.org/10.1038/s42005-018-0083-7), [1806.09826](https://doi.org/10.1038/s42005-018-0083-7).
- 240 [16] F. Schindler, A. M. Cook, M. G. Vergniory, Z. Wang, S. S. P. Parkin, B. A. Bernevig and  
241 T. Neupert, *Higher-order topological insulators*, Science Advances **4** (2018).
- 242 [17] A. Dutt, M. Minkov, I. A. Williamson and S. Fan, *Higher-order topological insulators in*  
243 *synthetic dimensions*, Light: Science and Applications **9**(1) (2020), doi:[10.1038/s41377-](https://doi.org/10.1038/s41377-020-0334-8)  
244 [020-0334-8](https://doi.org/10.1038/s41377-020-0334-8), [1911.11310](https://doi.org/10.1038/s41377-020-0334-8).
- 245 [18] W. Withayachumnankul, M. Fujita and T. Nagatsuma, *Integrated silicon photonic crystals*  
246 *toward terahertz communications*, Advanced Optical Materials **6**(16), 1800401 (2018),  
247 doi:[10.1002/adom.201800401](https://doi.org/10.1002/adom.201800401).
- 248 [19] R. A. S. D. Koala, M. Fujita and T. Nagatsuma, *Nanophotonics-inspired all-silicon wave-*  
249 *guide platforms for terahertz integrated systems*, Nanophotonics **11**(9), 1741 (2022),  
250 doi:[10.1515/nanoph-2021-0673](https://doi.org/10.1515/nanoph-2021-0673), Publisher: De Gruyter.
- 251 [20] T. Nagatsuma, G. Ducournau and C. C. Renaud, *Advances in terahertz com-*  
252 *munications accelerated by photonics*, Nature Photonics **10**(6), 371 (2016),  
253 doi:[10.1038/nphoton.2016.65](https://doi.org/10.1038/nphoton.2016.65).
- 254 [21] Y. Yang, Y. Yamagami, X. Yu, P. Pitchappa, J. Webber, B. Zhang, M. Fujita, T. Nagatsuma  
255 and R. Singh, *Terahertz topological photonics for on-chip communication*, Nature Photon-  
256 ics **14**(7), 446 (2020), doi:[10.1038/s41566-020-0618-9](https://doi.org/10.1038/s41566-020-0618-9), [1904.04213](https://doi.org/10.1038/s41566-020-0618-9).
- 257 [22] A. Kumar, M. Gupta, P. Pitchappa, N. Wang, M. Fujita and R. Singh, *Terahertz topological*  
258 *photonic integrated circuits for 6G and beyond: A Perspective*, Journal of Applied Physics  
259 **132**(14), 140901 (2022), doi:[10.1063/5.0099423](https://doi.org/10.1063/5.0099423).
- 260 [23] A. Leitenstorfer, A. S. Moskalenko, T. Kampfrath, J. Kono, E. Castro-Camus, K. Peng,  
261 N. Qureshi, D. Turchinovich, K. Tanaka, A. G. Markelz, M. Havenith, C. Hough *et al.*, *The*  
262 *2023 terahertz science and technology roadmap*, Journal of Physics D: Applied Physics  
263 **56**(22), 223001 (2023), doi:[10.1088/1361-6463/acbe4c](https://doi.org/10.1088/1361-6463/acbe4c).

- 264 [24] K. Kawase, Y. Ogawa, Y. Watanabe and H. Inoue, *Non-destructive terahertz imag-*  
265 *ing of illicit drugs using spectral fingerprints*, *Optics Express* **11**(20), 2549 (2003),  
266 doi:[10.1364/oe.11.002549](https://doi.org/10.1364/oe.11.002549).
- 267 [25] C. Jansen, S. Wietzke, O. Peters, M. Scheller, N. Vieweg, M. Salhi, N. Krumbholz, C. Jör-  
268 dens, T. Hochrein and M. Koch, *Terahertz imaging: Applications and perspectives*, *Applied*  
269 *Optics* **49**(19) (2010), doi:[10.1364/AO.49.000E48](https://doi.org/10.1364/AO.49.000E48).
- 270 [26] P. H. Siegel, *Terahertz technology in biology and medicine*, *IEEE Trans-*  
271 *actions on Microwave Theory and Techniques* **52**(10), 2438 (2004),  
272 doi:[10.1109/TMTT.2004.835916](https://doi.org/10.1109/TMTT.2004.835916).
- 273 [27] X. Yang, X. Zhao, K. Yang, Y. Liu, Y. Liu, W. Fu and Y. Luo, *Biomedical Applications*  
274 *of Terahertz Spectroscopy and Imaging*, *Trends in Biotechnology* **34**(10), 810 (2016),  
275 doi:[10.1016/j.tibtech.2016.04.008](https://doi.org/10.1016/j.tibtech.2016.04.008).
- 276 [28] J. F. Federici, B. Schulkin, F. Huang, D. Gary, R. Barat, F. Oliveira and D. Zimdars, *THz*  
277 *imaging and sensing for security applications - Explosives, weapons and drugs*, *Semicon-*  
278 *ductor Science and Technology* **20**(7) (2005), doi:[10.1088/0268-1242/20/7/018](https://doi.org/10.1088/0268-1242/20/7/018).
- 279 [29] Y. C. Shen, T. Lo, P. F. Taday, B. E. Cole, W. R. Tribe and M. C. Kemp, *Detection and*  
280 *identification of explosives using terahertz pulsed spectroscopic imaging*, *Applied Physics*  
281 *Letters* **86**(24), 1 (2005), doi:[10.1063/1.1946192](https://doi.org/10.1063/1.1946192).
- 282 [30] D. Marris-Morini, V. Vakarin, J. M. Ramirez, Q. Liu, A. Ballabio, J. Frigerio, M. Mon-  
283 tesinos, C. Alonso-Ramos, X. Le Roux, S. Serna, D. Benedikovic, D. Chrastina *et al.*,  
284 *Germanium-based integrated photonics from near- to mid-infrared applications*, *Nanopho-*  
285 *tonics* **7**(11), 1781 (2018), doi:[10.1515/nanoph-2018-0113](https://doi.org/10.1515/nanoph-2018-0113).
- 286 [31] M. Montesinos-Ballester, V. Vakarin, J. M. Ramirez, Q. Liu, C. Alonso-Ramos, X. Le Roux,  
287 J. Frigerio, A. Ballabio, A. Barzaghi, L. Deniel, D. Bouville, L. Vivien *et al.*, *Optical mod-*  
288 *ulation in Ge-rich SiGe waveguides in the mid-infrared wavelength range up to 11  $\mu$ m*,  
289 *Communications Materials* **1**(1), 8 (2020), doi:[10.1038/s43246-019-0003-8](https://doi.org/10.1038/s43246-019-0003-8).
- 290 [32] M. El Kurdi, S. David, X. Checoury, G. Fishman, P. Boucaud, O. Kermarrec, D. Bensahel  
291 and B. Ghyselen, *Two-dimensional photonic crystals with pure germanium-on-insulator*,  
292 *Optics Communications* **281**(4), 846 (2008), doi:[10.1016/j.optcom.2007.10.008](https://doi.org/10.1016/j.optcom.2007.10.008).
- 293 [33] M. Schatzl, F. Hackl, M. Glaser, P. Rauter, M. Brehm, L. Spindlberger, A. Simbula, M. Galli,  
294 T. Fromherz and F. Schäffler, *Enhanced telecom emission from single group-iv quantum dots*  
295 *by precise cmos-compatible positioning in photonic crystal cavities*, *ACS Photonics* **4**(3),  
296 665 (2017), doi:[10.1021/acsphotonics.6b01045](https://doi.org/10.1021/acsphotonics.6b01045).
- 297 [34] H.-J. Joo, Y. Kim, D. Burt, Y. Jung, L. Zhang, M. Chen, S. J. Parluhutan, D.-H.  
298 Kang, C. Lee, S. Assali, Z. Ikonic, O. Moutanabbir *et al.*, *1D photonic crystal direct*  
299 *bandgap GeSn-on-insulator laser*, *Applied Physics Letters* **119**(20), 201101 (2021),  
300 doi:[10.1063/5.0066935](https://doi.org/10.1063/5.0066935).
- 301 [35] C. V. Falub, H. Von Känel, F. Isa, R. Bergamaschini, A. Marzegalli, D. Chrastina,  
302 G. Isella, E. Müller, P. Niedermann and L. Miglio, *Scaling hetero-epitaxy from*  
303 *layers to three-dimensional crystals*, *Science* (80-. ). **335**(6074), 1330 (2012),  
304 doi:[10.1126/science.1217666](https://doi.org/10.1126/science.1217666).

- 305 [36] J. Pedrini, P. Biagioni, A. Ballabio, A. Barzaghi, M. Bonzi, E. Bonera, G. Isella and  
306 F. Pezzoli, *Broadband control of the optical properties of semiconductors through*  
307 *site-controlled self-assembly of microcrystals*, *Optics Express* **28**(17), 24981 (2020),  
308 doi:[10.1364/oe.398098](https://doi.org/10.1364/oe.398098).
- 309 [37] J. Pedrini, A. Barzaghi, J. Valente, D. J. Paul, G. Isella and F. Pezzoli, *Photonic Band*  
310 *Gap and Light Routing in Self-Assembled Lattices of Epitaxial Ge -on- Si Microstructures*,  
311 *Physical Review Applied* **16**(6), 1 (2021), doi:[10.1103/PhysRevApplied.16.064024](https://doi.org/10.1103/PhysRevApplied.16.064024).
- 312 [38] V. Falcone, A. Ballabio, A. Barzaghi, C. Zucchetti, L. Anzi, F. Bottegoni, J. Frige-  
313 rero, R. Sordan, P. Biagioni and G. Isella, *Graphene/Ge microcrystal pho-*  
314 *todetectors with enhanced infrared responsivity*, *APL Photonics* **7**(4) (2022),  
315 doi:[10.1063/5.0082421](https://doi.org/10.1063/5.0082421), 046106, [https://pubs.aip.org/aip/app/article-pdf/doi/10.](https://pubs.aip.org/aip/app/article-pdf/doi/10.1063/5.0082421/16492443/046106_1_online.pdf)  
316 [1063/5.0082421/16492443/046106\\_1\\_online.pdf](https://pubs.aip.org/aip/app/article-pdf/doi/10.1063/5.0082421/16492443/046106_1_online.pdf).
- 317 [39] Y. H. He, Y. F. Gao, H. Z. Lin, M. C. Jin, Y. He and X. F. Qi, *Topological edge and corner states*  
318 *based on the transformation and combination of photonic crystals with square lattice*, *Optics*  
319 *Communications* **512**(January), 128038 (2022), doi:[10.1016/j.optcom.2022.128038](https://doi.org/10.1016/j.optcom.2022.128038).
- 320 [40] B. Y. Xie, G. X. Su, H. F. Wang, H. Su, X. P. Shen, P. Zhan, M. H. Lu, Z. L. Wang  
321 and Y. F. Chen, *Visualization of Higher-Order Topological Insulating Phases in Two-*  
322 *Dimensional Dielectric Photonic Crystals*, *Physical Review Letters* **122**(23), 233903  
323 (2019), doi:[10.1103/PhysRevLett.122.233903](https://doi.org/10.1103/PhysRevLett.122.233903).
- 324 [41] X. D. Chen, W. M. Deng, F. L. Shi, F. L. Zhao, M. Chen and J. W. Dong, *Direct Observation of*  
325 *Corner States in Second-Order Topological Photonic Crystal Slabs*, *Physical Review Letters*  
326 **122**(23), 233902 (2019), doi:[10.1103/PhysRevLett.122.233902](https://doi.org/10.1103/PhysRevLett.122.233902), [1812.08326](https://arxiv.org/abs/1812.08326).
- 327 [42] K. H. Kim and K. K. Om, *Multiband Photonic Topological Valley-Hall Edge Modes and*  
328 *Second-Order Corner States in Square Lattices*, *Advanced Optical Materials* **9**(8), 1 (2021),  
329 doi:[10.1002/adom.202001865](https://doi.org/10.1002/adom.202001865).
- 330 [43] M. Makwana, R. Craster and S. Guenneau, *Topological beam-splitting in photonic crystals*,  
331 *Optics Express* **27**(11), 16088 (2019).
- 332 [44] F. Isa, M. Salvalaglio, Y. A. R. Dasilva, M. Meduña, M. Barget, A. Jung, T. Kreiliger,  
333 G. Isella, R. Erni, F. Pezzoli, E. Bonera, P. Niedermann *et al.*, *Highly Mismatched,*  
334 *Dislocation-Free SiGe/Si Heterostructures*, *Advanced Materials* **28**(5), 884 (2016),  
335 doi:[10.1002/adma.201504029](https://doi.org/10.1002/adma.201504029).
- 336 [45] F. Montalenti, F. Rovaris, R. Bergamaschini, L. Miglio, M. Salvalaglio, G. Isella, F. Isa  
337 and H. V. Känel, *Dislocation-Free SiGe/Si Heterostructures*, *Crystals* **8**(257), 1 (2018),  
338 doi:[10.3390/cryst8060257](https://doi.org/10.3390/cryst8060257).
- 339 [46] R. Bergamaschini, F. Isa, C. V. Falub, P. Niedermann, E. Müller, G. Isella, H. Von Känel  
340 and L. Miglio, *Self-aligned Ge and SiGe three-dimensional epitaxy on dense Si pillar arrays*,  
341 *Surface Science Reports* **68**(3-4), 390 (2013), doi:[10.1016/j.surfrep.2013.10.002](https://doi.org/10.1016/j.surfrep.2013.10.002).
- 342 [47] F. Pezzoli, F. Isa, G. Isella, C. V. Falub, T. Kreiliger, M. Salvalaglio, R. Bergamaschini,  
343 E. Grilli, M. Guzzi, H. Von Känel and L. Miglio, *Ge Crystals on Si Show Their Light*,  
344 *Physical Review Applied* **1**(4), 1 (2014), doi:[10.1103/PhysRevApplied.1.044005](https://doi.org/10.1103/PhysRevApplied.1.044005).
- 345 [48] F. Pezzoli, A. Giorgioni, K. Gallacher, F. Isa, P. Biagioni, R. W. Millar, E. Gatti, E. Grilli,  
346 E. Bonera, G. Isella, D. J. Paul and L. Miglio, *Disentangling nonradiative recombination*  
347 *processes in Ge micro-crystals on Si substrates*, *Applied Physics Letters* **108**(26) (2016),  
348 doi:[10.1063/1.4955020](https://doi.org/10.1063/1.4955020), [1603.08700](https://arxiv.org/abs/1603.08700).

- 349 [49] T. Amotchkina, M. Trubetskov, D. Hahner and V. Pervak, *Characterization of e-beam evap-*  
350 *orated ge, ybf3, zns, and laf3 thin films for laser-oriented coatings*, Applied Optics **59**(5),  
351 A40 (2020), doi:[10.1364/AO.59.000A40](https://doi.org/10.1364/AO.59.000A40).
- 352 [50] *Comsol multiphysics® v. 5.6.*, [www.comsol.com](http://www.comsol.com). comsol ab, stockholm, sweden.
- 353 [51] J. D. Joannopoulos, *Photonic Crystals: Molding the Flow of Light*, Princeton University  
354 Press, 2 edn., ISBN 978-0691124568 (2008).
- 355 [52] G. Dehlinger, L. Diehl, U. Gennser, H. Sigg, J. Faist, K. Ensslin, D. Grützmacher and  
356 E. Müller, *Intersubband electroluminescence from silicon-based quantum cascade structures*,  
357 Science **290**(5500), 2277 (2000), doi:[10.1126/science.290.5500.2277](https://doi.org/10.1126/science.290.5500.2277).
- 358 [53] D. J. Paul, *The progress towards terahertz quantum cascade lasers on silicon substrates*,  
359 Laser and Photonics Reviews **4**(5), 610 (2010), doi:[10.1002/lpor.200910038](https://doi.org/10.1002/lpor.200910038).
- 360 [54] W. P. Su, J. R. Schrieffer and A. J. Heeger, *Solitons in polyacetylene*, Physical Review  
361 Letters **42**(25), 1698 (1979), doi:[10.1103/PhysRevLett.42.1698](https://doi.org/10.1103/PhysRevLett.42.1698).
- 362 [55] F. Liu and K. Wakabayashi, *Novel Topological Phase with a Zero Berry Curvature*, Physical  
363 Review Letters **118**(7), 1 (2017), doi:[10.1103/PhysRevLett.118.076803](https://doi.org/10.1103/PhysRevLett.118.076803), [1711.08712](https://doi.org/10.1103/PhysRevLett.118.076803).
- 364 [56] A. B. Khanikaev and G. Shvets, *Two-dimensional topological photonics*, Nature Photonics  
365 **11**(12), 763 (2017), doi:[10.1038/s41566-017-0048-5](https://doi.org/10.1038/s41566-017-0048-5).
- 366 [57] Y. Gong, S. Wong, A. J. Bennett, D. L. Huffaker and S. S. Oh, *Topological in-*  
367 *insulator laser using valley-hall photonic crystals*, ACS Photonics **7**(8), 2089 (2020),  
368 doi:[10.1021/acsp Photonics.0c00521](https://doi.org/10.1021/acsp Photonics.0c00521).
- 369 [58] M. I. Shalaev, W. Walasik, A. Tsukernik, Y. Xu and N. M. Litchinitser, *Robust topologi-*  
370 *cally protected transport in photonic crystals at telecommunication wavelengths*, Nature  
371 Nanotechnology **14**(1), 31 (2019), doi:[10.1038/s41565-018-0297-6](https://doi.org/10.1038/s41565-018-0297-6).
- 372 [59] B. Y. Xie, H. F. Wang, H. X. Wang, X. Y. Zhu, J. H. Jiang, M. H. Lu and Y. F. Chen,  
373 *Second-order photonic topological insulator with corner states*, Physical Review B **98**(20),  
374 1 (2018), doi:[10.1103/PhysRevB.98.205147](https://doi.org/10.1103/PhysRevB.98.205147), [1805.07555](https://doi.org/10.1103/PhysRevB.98.205147).
- 375 [60] L. Zhang, Y. Yang, Z. K. Lin, P. Qin, Q. Chen, F. Gao, E. Li, J. H. Jiang, B. Zhang and  
376 H. Chen, *Higher-Order Topological States in Surface-Wave Photonic Crystals*, Advanced  
377 Science **7**(6) (2020), doi:[10.1002/advs.201902724](https://doi.org/10.1002/advs.201902724).
- 378 [61] J. Bravo-Abad, A. Rodriguez, P. Bermel, S. G. Johnson, J. D. Joannopoulos and M. Sol-  
379 jačić, *Enhanced nonlinear optics in photonic-crystal microcavities*, Optics Express **15**(24),  
380 16161 (2007), doi:[10.1364/OE.15.016161](https://doi.org/10.1364/OE.15.016161).
- 381 [62] F. Gao, H. Xue, Z. Yang, K. Lai, Y. Yu, X. Lin, Y. Chong, G. Shvets and B. Zhang, *Topologi-*  
382 *cally protected refraction of robust kink states in valley photonic crystals*, Nature Physics  
383 **14**(2), 140 (2018), doi:[10.1038/nphys4304](https://doi.org/10.1038/nphys4304), [1706.04731](https://doi.org/10.1038/nphys4304).